Research Square

Preprints are preliminary reports that have not undergone peer review.
They should not be considered conclusive, used to inform clinical practice,
or referenced by the media as validated information.

Development And Synthesis Of Piezoelectric Materials Based On Natural Resources (Rocks)

Noura Mebrouki (mebroukinoura4@gmail.com)
Univ Ouargla
Louiza Zenkhri
Univ Ouargla
Salah Tlili
Univ Ouargla
Souhila Boudjemaa
Univ Tlemcen
Hakim Belkhalfa
Univ Ouargla, Scientific and Technical Research Center in Physico-Chemical Analysis (CRAPC)
Lazhar Benmabrouk
Univ Ouargla

Research Article

Keywords: Sand stone, thin film, glass substrat, piezoelectric, hydrothermal synthesis

Posted Date: September 7th, 2022

DOI: https://doi.org/10.21203/rs.3.rs-2022041/v1

License: This work is licensed under a Creative Commons Attribution 4.0 International License.
Read Full License

Abstract

This study reports the chemical composition of seven sandstones (OH1-OH7) from Ouargla desert in south-east of Algeria, then the investigation of these samples to be used as precursor for the hydrothermal synthetesis of piezoelectric mater in thin films form. Fourier-transform infrared (FT-IR) spectra shows the characteristic vibration bond peaks for the seven samples documenting the presence of quartz and calcite. Moreover, chemical composition of Ouargla sandstones has been determined by energy dispersive X-ray (EDS) and X-ray diffraction (XRD) allowed mainly a composition avrage major of 86.86 % α-quartz (SiO_2) and minor of 13.14 % calcite ($CaCO_3$). The EDS analysis revealed the presence of solid solution in the crystal lattice of six samples of the sandstones with trace amounts of Fe, Al, Ag, Na, K. The aqua regia digestion method was used to extract silicon and calcium from the rock samples in to synthesis the thin films. From (FT-IR), (SEM-EDS) and (XRD) we show that synthesis thin films at different temperture are composed mainly of 90.66 % calcite ($CaCO_3$)/9.33 % α-quartz (SiO_2) and 69 % α-quartz (SiO_2)/31% Sodium Chloride (NaCl). The crystallite sizes of the sandstones were calculated and estimated to be nanometric, in contrast the thin films are not nanometric.

Introduction

The humain have alwayshad arelationshipwith rocks.Rocks are foundeverywhere on the globe: deserts, mountains, beaches. Also, it was noticed in the vast deserts that there are many minerals and natural resources (rocks) with a special geological source, and these minerals have received some geomorphological geological studies that have been concerned with studying the shapes and types of rocks [1],where is the last one on earth can appear with endless array of colors, started from shiny bright and ended with dull dark. The variety of their colors is a result of number of factors [2].The rocks which constitute the earth's crust are considered as origin of minerals, Consisting essentially of assemblage of various minerals. They can be broadly classified, depending on their mode of origin, into three major divisions: The sedimentary, metamorphic and igneous rocks [3].Sedimentary rocks are made up of a very small selection of mineral sun like the igneous rocks, viz quartz, carbonates, clay and feld spars. Minerals are the foundations of industries ranging from constructions, manufacturing, agricultural technology to cosmetics [4].

Why is rock research interesting in general? In order to gain interest in the current field of research. It is interesting to do research in rocks for multiple objectives in the field of geophysics, geology, or in the field of earth sciences. The rocks are studied to identify the formation of specific regions or to know the stability of a particular region, such as being affected by environmental problems like radiation [5]. Several studies have been made in many countries to determine the concentration of the natural radionuclides in rock samples [6].In materials science or material physics, the characteristics of rocks has been investigated with various methods [7, 8, 9] in micro structure as well as macro structure which can describe the physical properties of rocks [10, 11], and structural properties [5, 12, 13, 14]. Moreover, the information about mineral of rocks will provide the properties of rocks [15].

Calcium carbonate ($CaCO_3$) is one of the world's most abundant materials and has several different crystalline forms calcite, aragonite and vaterite [16]. The orthorhombic polymorph of $CaCO_3$, continues to attract the attention of researchers 95 years after its first structure determination by W. L. Bragg in1924 [17]. This is due to the widespread abundance of aragonite and its important role in geochemistry and especially in biomineralization [18].The calcite structure has the space group R3c [19], it's thin film has been fabricated by several methods as reports in [20, 21, 22]. Calcite is important in sedimentary environments and occurs in metamorphic and igneous, as well as in hydrothermal and secondary mineralization. Aragonite and calcite are of interest because they occur in various geological environments [23].These calcite-type minerals are often used as model compounds for investigating structural sources of optical anisotropy [19].

Silicon and oxygen the two components of quartz (SiO_2) are two of the most abundant elements in the Earth's crust. Quartz occurs in two phases of polymorphs: α-quartz or β-quartz [24]. Quartz is present in rocks, soils, and sands and forms from molten magma at ~800 ºC and underground hydrothermal veins at temperatures from 250 to 450 ºC [25]. According to the literature, quartz thin films can be prepared by several methods [26, 27, 28].Chemically, quartz is very close to 100% SiO_2 and only a few elements can be incorporated into its crystal lattice [29, 30, 31, 32]. Due to the wide spread occurrence of quartz in igneous, metamorphic and sedimentary rocks, several attempts have been made to use trace elements for genetic interpretations [33, 34, 35, 36].

Among the materials used for high precision transducers and sensors industry based on bulk acoustic waves, conventional piezoelectric materials such as quartz is widely used. However, their operating temperature is limited by the material properties at about 500 °C. High temperature applications are achievable by applying materials that retain their piezoelectric properties up to higher temperatures [37]. Among the properties of quartz is its piezoelectric properties [27], which has been investigated through a study of the converse piezoelectric effect. In the case of quartz, the piezoelectric constant has been measured from point to point across the specimen [38]. Also, the piezoelectric effects was discovered in rocks by M.P. Volarovich and E.1. Parkhomenko in 1954 [39]. Also, A. V. Shubnikov explained the piezoelectric effect in polycrystals (rocks) on the basis of theory proposed [40]. The piezoelectric effect of rocks is widely used in geophysics. Unfominately, in our knowldge no theory or statistical model on the formation of piezoelectric active texturized rocks exists yet. This is due to the lack of experimental information and due to restricted knowledge how the piezoclectric properties of rocks are related to the conditions and mechanisms of rock genesis [41].

The goal of this work was the exploitation of natural resources (rocks) to be used as precursors for the hydrothermal synthesis of piezoelectric material in thin films form in the futur, since it contains expensive chemical elements and is not harmful to health and no-polluting to the environment.

Description of the study area

Algeria has the largest area in Africa, it has a variety of terrains, geology and vast amounts of rocks rich in large mineral reserves that can be mined. The Ouargla region is known for the presence of some rocky stones of different colors on its bottom, which have been recovered approximately 3 to 5 cm in length. The study site is on the road that connects the two cities of Ouargla and Hassi Messaoud. The zone is delimited by the longitude 5° 20’ E and the latitude 31° 57’ N exactly in the geographical position (31.802505.5395) with an average height of 137 m [42]. It is geographically located in north-eastern Algeria, more precisely in the northern part of the Algerian Sahara. It is characterized by high temperatures.

Expermental Methods

Rock Collecting

The rocks (Fig. 2) were sampled in 2019 from the same region between Ouargla and Hassi Messaoud (OH) that exist on the surface. They were of different size, color and irregular shape, Fig. 2.

The seven sandstones (OH1- OH7) were used as the source of metallic cations. Serium carbonate $SrCO_3$ was obtained from (BIOCHEM), HNO_3 (65%), HCl (37%) and distilled water. The substrates used to support the formed thin film were (0382-0004) Cito glass slides with a size of ($75 \times 25 \times 1.1\ mm^3$).

Rock Pollishing and Grinding

The collected rocks were washed, pollished to removes some impurities by using Mecapol P 255 U device and thoroughly dried at room temperature, then crushed using Retsch device for few minutes and (V= 950 rpm) to obtain a fine powder. Finaly the powder kept in a plastic box for after use.

Synthesis of ($CaCO_3$-SiO_2) thin films

The powdered rock samples with a mass of about 3 mg was soaked for 48 hours in mixture of 3 ml HNO_3 and 9 ml of HCl (aqua regia) at room temperature After two days we extracted it. Then we took only 3 ml of it and extension by 15 ml of distilled water with 3 mg Serium carbonate ($SrCO_3$). The resulting mixture was put inside astainless-steel hydrothermal reactor which is containe a glass substrat at 150 °C, 200 °C, 250 °C and 300 °C respectively. After 2 hours the reactions mixture were cooled down at room temperature and the products were filtered off and washed with distilled water and aciton several times.

Fourier-Transform Infrared (FTIR) technique

Infrared spectroscopy (FTIR) is a simple method which can be used to identify the chemical bands from the organic, inorganic, crystalline or amorphous compound [43]. The FTIR measurements were carried out using a Agilente cary 660 FTIR spectrometer. The samples were scanned in a spectral range from 4000 to 400 cm^{-1}.

Scanning electron microscopy (SEM-EDS) technique

Sample of the natural sandstones powder and the morphology of the $CaCO_3/SiO_2$ thin films were subjected to SEM-EDS analysis using TESCAN VEGA3 electron microscope.

X-rays diffraction identification

X-rays cristallgraphic data were collected on powdered samples at room temperature using a powder diffractometer BTX-716 and BRUKER-binary V3 with Cu Kα radiation at the wavelenght (λ = 1,5406 Å) radiation at room temperature, operating voltage 40, 35 KV and electric current 40, 30 mA, respectivelly. All samples were analysed from 5° to 55° and from 20° to 90° by a step of 0.0500 °/s, 0.019 °/s respectivelly, and 250 exposures. The phasis structures were identified using the expert High Score Plus softward [44] configured with ASTM file.

Results

Characterisation of rocks

Fourier-Transform Infrared (FTIR) analysis

Form FTIR qualitative analysis, and by comparing our results with other studies, the obtained vibration bonds values are in good agreement with results carried out in the literature [45, 46, 47] which indicates that the most bands are attributed to quartz and calcite. Fig. 3 and Table 1 show FTIR spectra of the OH sandstones. This is consistent with the XRD results. The peaks of absorption observed between 425.14-429.47, 440.49-449.81 cm^{-1}, 467.13-483.19 cm^{-1}, 693.91-694.004 cm^{-1}, 777.17-798.38 cm^{-1} presented in Fig. 3 indicate the presence of quartz in all rock samples. The characteristic peaks between 1081.85-1096.83 cm^{-1} and 2357.08-2361.79 cm^{-1} indicating the emergence of calcite in the whole samples except OH7 the last peaks were absent [45, 48].

Table 1. The main bands of IR absorption and associated bond vibration of our samples.

Band(cm−1)	Bond (vibration mode)	Compound
2357.08-2361.79	indicating the emergence of calcite	Calcite
1081.85-1096.83	Si–O–Si (symmetrical stretching)	Quartz
1088	indicating the emergence of calcite	Calcite
1090	vibrations of the carbonate ions	Calcite
777.17-798.38	Si-O (symmetrical bending vibration)	Quartz
693.91-694.004	Si–O–Si (symmetrical bending)	Quartz
694.004	Quartz	Quartz
467.13-483.19	Si-O (symmetrical streching)	Quartz
440.49-449.81	Si-O-Si (asymmetrical bending)	Quartz
425.14-429.47	Si-O-Fe (bending vibrations)	Quartz

Elemental analysis (EDS)

The element concentrations obtained for the seven sandstones (OH1-OH7) are summarized in the Table 2. The presence of the identical substantial elements (O, Si, C, Ca) in all the samples is a clear indication of the natural quartz/calcite structure of the rocks. While the specific trace metal (Fe, Al, Ag, Na, K) for each sample, with significant differences observed in their presence and concentrations shows that the quartz/calcite structure might be modifie. Shanling, Qing and Jun have reported in their work that data study of trace element distribution in hydrothermal quartz from southern China reveal that Al, Li, Na, and K are the most important elements in quartz [55], while Fe also can be embedded in the crystal lattice of calcite [56]. The variety of chemical composition for the seven rock can explain the differences of their colors.

Table 2. Elemental analysis of OH sandstones.

Samples	O (%)	Si (%)	C (%)	Fe (%)	Al (%)	Ag (%)	Na (%)	K (%)	Ca (%)
OH1	66.58	21.65	9.97	0.85	0.55	0.41			
OH 2	67.69	31.28		0.36	0.67				
OH 3	61.83	25.39	9.48	1.70	1.13		0.47		
OH 4	61.88	22.86	11.94	1.75	0.89				0.68
OH 5	68.66	24.51		0.74	2.98		1.77	0.90	0.44
OH 6	61.32	36.69		1.20	0.35				0.44
OH 7	61.87	1.46	19.54						17.14

X-ray diffraction (XRD) analysis

XRD studies were done to estimate the qualitative and quantitative phase analysis of the OH sandstones to determine the rock structure. In the measured XRD, a strong diffraction peaks could be seen, indicating that OH sandstones have high crystalline nature, which agrees with the results of Meftah and Mahboub 2020 [57]. The results of the Xpert HighScore software matching revealed the presence of quartz in the majority and calcite in the rock samples as shown in Fig. 4 and Table 3.

Table 3. Indexed Powder XRD Pattern for OH sandstones.

2θ(°)	Intensity(a.u)	Mineral	(dhkl) cal (Å)	Hkl
20.7709	1556.38	Quartz	4.27305	100
26.5832	5789.14	Quartz	3.35048	101
29.2773	443.325	Calcite	3.04801	104
31.5967	324.419	Calcite	2.82935	006
35.8935	279.252	Calcite	2.49989	110
36.4035	635.429	Quartz	2.46603	110
39.3111	682.268	Quartz, Calcite	2.29007	102/113
40.2535	385.766	Quartz	2.23860	111
42.3029	555.187	Quartz	2.13477	200
47.1143	244.788	Calcite	1.92737	024
48.6941	221.515	Calcite	1.86847	116
49.9412	613.894	Quartz	1.82469	112

Table 4. Lattice parameters a, c and crystalline size D of quartz and calcite of OH sandstones.

Mineral	Standard lattice parameters (Å)	Calculated lattice parameters (Å)				FWHM (°)	Crystalline sizes (nm) (D)
		a	Δa = a0-a	c	Δc = c0-c		
Quartz (SiO_2)	a0 = 4.9134[a]	4.93206	-0.0187	5.4741	−0.0689	0.18	35.44
	c0 = 5.4052[a]						
Calcite ($CaCO_3$)	a0 = 4.9890[b]	4.99978	-0.01078	16.9761	0.0859	0.36	43.4
	c0 = 17.0620[b]						

[a]data from JCPDS (N° 46–1045)

[b]data from JCPDS (N° 05–0586)

The d_{hkl} inter-planar spacing has been calculated from the X-ray diffraction profile using the Bragg law:

$$2d_{hkl}\sin\theta = n\lambda \quad (1)$$

Where θ is the diffraction angle, λ is the used wavelength of X-rays and n is the order of diffraction. We note that the calculated value of d_{hkl}-spacing (Table 3) matched very well with those of the standard JCPDS data. The lattice constants a, b and c, for the hexagonal and rhombohedral phase structure were determined from XRD results using the following equation [64]:

$$\frac{1}{d_{hkl}^{\ 2}} = \frac{3}{4}\left(\frac{h^2+hk+k^2}{a^2}\right) + \frac{1}{c^2}^{\ 2} \quad (2)$$

Where (h k l) are the Miller indexes and 'a', 'c' are the lattice constants. The calculated and standard JCPDS lattice constants for quartz and calcite are indicated in Table 4. As we can see, the calculated lattice parameters for the quartz (a = b = 4.93206 Å and c = 5.4741 Å) and calcite (a = b = 4.99978 Å and c = 16.9761 Å) agree well with the standard values (a_0 and c_0). We can further calculate the crystallite sizes D of the quartz and calcite of our rocks from the strongest peaks by using Scherrer's formula [65]:

$$D = \frac{0.96\lambda}{\beta\cos\theta} \quad (3)$$

Where D is the crystallite size, λ (=1.5406 Å) is the wavelength of X-rays, β is the width full at half maximum (FWHM) of the most intense diffraction peak, usually measured in radian and θ is the Bragg angle.

Synthesis

Fourier-Transform Infrared (FTIR) analysis

Fig. 5 and Table 5 show FTIR spectra of the thin films synthesised at 150 °C, 200 °C, 250 °C and 300 °C. The bands of absorption observed at 428.11, 524.54 and 983.73 cm^{-1} are indicate the presence of quartz in all thin films [52, 53, 54, 66]. The other characteristic peaks at 711.60, 875.52, 1430.92 and 2354.66 cm^{-1} attributed to the CO_3^{-2} ion, indicating the presence of calcite in the whole thin films [48, 50, 66].

Table 5. The main bands of IR absorption and associated bond vibration of our thin films.

Wavenumber (cm^{-1})		Assignement
Calcite	Quartz	
	428.11	Si-O-Fe bending vibrations
	524.54	Si-O-Al asymmetrical vibrations
711.60		CO_3^{-2} (in-plane bending)
875.52		CO_3^{-2} (out-of-plane bending)
983.73		The vibration of quartz
1430.92		CO_3^{-2} Asymmetrical stretching vibrations
2354.66		Calcite

Morphological analysis (SEM)

Fig. 6 shows SEM surface images of the calcite-quartz thin films synthesized on the glass substrate at different temperatures. In Fig. 2 a, c, d, when the temperature was 150 °C, 250 °C and 300 °C, the surface morphologies of the $CaCO_3$ thin films are thin, wool-like bristles, circular disk-shaped and of unspecified thickness and scattered pieces with irregular structure, respectively. While the SiO_2 thin films at 150 °C, 200 °C and 300 °C are a substance in the form of grains and have approximately the same size of particles that reflect light, while SiO_2 at 250 °C has a mass of particles with approximately different size. At 200 °C, the NaCl thin films are a regular particle with a smooth surface. We conclude that the optimal temperature to obtain a thin calcite films is 250 °C and the morphology of our films prepared by hydrothermal synthesis is temperature dependent.

Elemental analysis (EDS)

Table 6. Showed EDS results representative peaks for O, Si, and Ca for all the samples at 150 °C, 200 °C and 300 °C. The EDS of the synthesised film at 150 °C consists mainly of O (69.267%), Si (14.521%), Mg (5.065 %), Ca (4.476 %) and Al (0.963 %), while at 200 °C : O (30.278 %), Na (22.156 %), Si (15.796 %), P (13.351 %), Ca (8.466 %), Ag (5.186 %), Al (2.392 %) and Mg (2.376 %). Whereas at 300 °C : O (69.594%), Si (10.161%), Na (8.418 %), Mg (6.649 %), Ca (2.601%), P (1.512 %), Ag (0.581 %) and Al (0.484 %).

The CaCO3/SiO2 thin films show similar peaks corresponding to the spectra of SiO2/CaCO3, which indicate a successful formation of CaCO3/SiO2 thin films.

Table 6. Elemental analysis of synthesis thin films at different temperatures.

Thin films	O %	Si %	Ca %	Na %	Al %	Ag %	Mg %	P %
150°C	69.267	14.521	4.476	5.503	0.963	0.205	5.065	
200°C	30.278	15.796	8.466	22.156	2.392	5.186	2.376	13.351
300°C	69.594	10.161	2.601	8.418	0.484	0.581	6.649	1.512

X-ray diffraction (XRD) analysis

XRD patterns of the thin films formed at different temperatures are presented in Fig. 7. This figure shows that the observed peaks at 150 °C, 250 °C and 300 °C are matched with ASTM file (N° 00-005-0586) and (N° 00-046-1045) forms the ($CaCO_3$/SiO_2) with ratio (98/2), (89/11) and (85/15) respectively. Furthermore, at 200 °C forms the (SiO_2/NaCl) ASTM file (N° 00-005-0628) with (69/31) ratio.

Discussion

Fourier-Transform Infrared (FTIR) analysis

The sharp absorption band between 1081.85-1096.83 cm^{-1} has been observed and seems to fit with symmetrical stretching of Si–O–Si bond [47, 49, 50]. *CHENGLI YAO (2013) and Flemming A. Andersen* (1991) have *reported the c*haracteristic peaks at 1088 and 1090 cm^{-1}, indicating the emergence of calcite [48], and the vibrations of the carbonate ions [50], respectively. Whereas the absorption bands between 777.17-798.38 cm^{-1} have been observed and correspond to Si-O symmetrical bending vibration, which confirm the presence of α-quartz [46, 47]. In addition, we observed other bands between 693.91-694.004 cm^{-1} which coincide with Si–O–Si symmetrical bending. These peaks confirm again the presence of quartz in our samples. The 694.004 cm^{-1} band indicates that the quartz in the samples is crystalline [51]. The absorption peaks between 500-530 cm^{-1}, 467.13-483.19 cm^{-1}, 440.49-449.81cm^{-1} and 425.14-429.47 cm^{-1} due to the asymmetrical vibrations of Si-O-Al, symmetrical streching of the Si-O, asymmetrical bending of the Si-O-Si band and bending vibrations of Si-O-Fe, respectively [47, 52, 53, 54].

X-ray diffraction (XRD) analysis

By matching the observed XRD peaks (Fig. 4) with ASTM cards, some notes can be recorded:

The peaks positioned at 2θ =20.7709°, 26.5832°, 36.4035°, 39.3111°, 40.2535°, 42.3029° and 49.9412° corresponding, respectively, to the planes (100), (101), (110), (102), (111), (200) and (112) are due to the hexagonal crystal structure of SiO_2 (α-quartz), under the space group P3221 (154) which is consistent with JCPDS file (N° 00-046–1045) [57] with a lattice parameters of a = b = 4.9134 Å and c = 5.4052 Å. Whereas diffractions at 2θ= 29.2773°, 31.5967°, 35.8935°, 39.3111°, 47.1143° and 48.6941°, for the crystalline planes (104), (006), (110), (113), (024) and (116), respectively. These planes fit calcite ($CaCO_3$)

compound as reported by JCPDS (N° 00-005-0586) with a rhombohedral crystal system belonging to R3c (167) space group [58, 59, 60] with a = b = 4.99978 Å and c = 16.9761 Å.

Quartz is characterized by its strongest, highest intensity and prominent diffraction at 2θ = 26.5832° c

From Table 3 the spacing distances d_{hkl} of 4.27305, 3.35048 and 2.46603 (Å) / 3.04801, 2.82935 and 2

The crystallite size of quartz D = 19.94 (OH1), 35.44 (OH2), 24.66 (OH3), 24.79 (OH4), 33.80 (OH5), 25.24 (OH6), 26.33 (OH7) nm whereas the crystallite size of calcite D = 13.85 (OH1), 43.40 (OH2), 22.88 (OH3), 30.75 (OH4), 38.18 (OH5), 41.48 (OH6), 27.65(OH7) nm, both of them remain less than 100 nm which makes it of great interest to the nanometric industries and nanotechnologies.

Synthesis

Fourier-Transform Infrared (FTIR) analysis

The peaks at 428.11, 524.54 and 983.73 cm^{-1} are assigned, respectively, to Si-O-Fe, Si-O-Al lattice flexing vibrations [52] and bending vibrations [53, 54] and the absorption band at 983.73 cm^{-1} attributable to the vibration of quartz [66]. The absorption band at 2354.66 cm^{-1} is specified at 150 °C, its mode of movoument vibrations of the band was not specified [48]. The absorption band at 1430.92 cm^{-1} refers to the asymmetrical stretching vibrations of the carbonate ion CO_3^{-2}, while the 875.52 cm^{-1} band is assigned to the out-of-plane bending, whereas, the 711.60 cm^{-1} band is assigned to its in-plane bending [66].

X-ray diffraction (XRD) analysis

Whereas, the reaction temperature increased to 250 °C then to 300 °C, the intense peaks at 2θ = 29.4104° (150 °C) of the calcite phase [61] has shifted to 31.67. This is an expected shift given the traces elements anchored to the crystal lattice previously reported by SEM-EDS analysis as different types and values, and this may be the slight too to the deformation of the crystal lattice due to temperature. By the same, at 150 °C the pattern exhibited the peak diffraction (2θ) near 36.0435 of the calcite cristallization, while at 250 °C (36.4899) and 300 °C (36.4412) reflect to quartz. The the peak at 2θ =39.0435° (150 °C), 39.4120° (250 °C) and 39.6531° (300 °C), respectively, reflect the existence of calcite as reports in [60, 62] and the existence of quartz phases at the same time as reports in [67, 68]. There are also another peaks for quartz / calcite 42.3904° (150 °C) 42.1719°/47.1827° (250 °C), 42.4828°/43.2101° (300°C), 59.9443°, 67.7348° and 80.6060° (200°C). At 200°C the thin films also contains NaCl which exhibits two intense peaks at 2θ = (31.7266° and 66.1949°). These two peaks correspond respectively to the (200) plane and its harmonic (400) are due to the cubic system with the Fm3m symmetry space group as reported in the JCPDS (N° 00-

005-0628 card) [69] with a = b = c = 5.636176 Å. While the decrease in the intensity of the peaks when the heat of reaction increases indicates that the good crystallization takes place at 150 °C.

The results show the synthesis of the thin films of calcite and quartz at reaction's different temperature, except that at 200 °C there is no calcite present. The presence of specific trace metals for each sample, with significant differences observed in their presence and concentrations, indicates that the quartz/calcite structure may be modified as reported in the previous analysis (EDS) and this may be the slight Shift in explained position of the spectra due to different radii from mineral bead to mineral bead.

The crystallite size of quartz D = 113.63 (150 °C), 116.05 (200 °C), 101.27 (250 °C), 109.07 (300 °C) nm whereas the crystallite size of calcite D = 65.68 (150 °C), 101.98 (250 °C), 121.77 (300 °C) nm and the crystallite size of Sodium Chloride D = 97.08 (200 °C) nm, Therefore, the quartz and calcite thin films are not nanometric at all reaction temperatures, except that at 150 °C the calcite thin films and at 200 °C the Sodium Chloride thin films are less than 100 nm, making them of great interest to the nanometric industries and nanotechnologies.

Conclusion

- As far as the literature is known, this is the first study of the OH sandstones region, which develops them as precursors for the hydrothermal synthesis of piezoelectric material in the thin films form while preserving the crystal lattice by transformation the solid particles attached to each others into thin films that can be used in nanometric industries and nanotechnologies.

- By using XRD analysis, SEM-EDS and FTIR spectroscopy we found that OH sandstones mainly consists of about 86.86% quartz in α- phase, minor calcite mineral (about 13.14%) and some trace elements (Al, Fe, Na, Ag, K), this indicates a high purity of the quartz and calcite of these sandstones and their thin films.

- OH sandstones are very rich in quartz with hexagonal crystal structure with space group P3221 (154). In addition, the rock has some calcite with a rhombohedral crystal system with space group R3c (167), which has been authenticated by XRD analysis.

- The most intense peaks are 26.5832 and 29.4104 corresponding to (101) and (104) respectively, these planes indicating the preferential orientation of quartz and calcite growth in these sandstones and thin films.

- XRD has been used for the qualitative and quantitative analysis of multi-component mixtures such as rocks, which is the most commonly used technique.

- OH sandstones could be important sources of quartz and calcite which are primary materials for many industrial applications such as glass fabrication, semiconductors and optical anisotropy. In addition, rock has a great importance in many fields of science, earth sciences, geophysics and geology.

- The characteristic vibration bond peaks indicate the existence of quartz in OH sandstones, with low concentrations of calcite. On the contrary, the most vibration bonds are attributed to calcite in thin films, with low concentrations of quartz. This is consistent with the XRD results.

- The crystallite sizes of quartz and calcite are D = 27.17 and 31.17 nm, respectively, demonstrating the nanometric aspect of the OH sandstones.

- The variety of sandstones colors is directly related to their chemical composition and the traces of metal they contain.

- After the success of converting the nanoscale raw material ($SiO_2/CaCO_3$) into a non-nanoscale thin film, as a future prospect, we will try to improve the particle size of the thin films to successfully produce them from a natural material by changing the experimental conditions, to make quartz thin films on a nanoscale and with piezoelectric properties from natural precursor rocks known to possess these properties, which can not be used in the industrial and nanotechnology fields, and therefore transform them to thin films can be used. Since for calcite, 150 °C or less is considered optimum to obtain nano-scale thin calcite thin films which were nanometer crystal grains. At 250 °C, calcite was a continuous thin film, cohesive and crystallized, but not on a nanoscale, the development of thin films.

Abbreviations

OH : Ouargla-Hassi Messaoud

FT-IR : Fourier-Transform Infrared

EDS : Energy dispersive X-ray

SEM : Scanning electron microscopy

XRD : X-ray diffraction

Cu Kα : Anode radiation

KV : Kilo Volts

°C : Temperature

nm : nanometer

A°: Angström

θ : The diffraction angle

λ : The used wavelength

n : The order of diffraction

d_{hkl} : Inter-planar spacing

(h k l) : The Miller indexes

‘a’, ‘c’ : The lattice constants

D: The crystallite size

β: The width full at half maximum (FWHM)

Declarations

Acknowledgments

The authors gratefully acknowledge the assistance of everyone in the completion of this work. Sincere thanks are extended to Pr. Gheriani Rachid and Pr. Hesseni Messoud. Thin film laboratory, Mohamed Khider University of Biskra, Algeria; Sahara geology laboratory (E1521600) Address BP 511 avenue of Ghardaia, Ouargla, Algeria; the Center for Scientific and Technical Research in Physico-chemical Analysis (CRAPC) Ouargla, Algeria; Lab. DAC-HR University of Setif 1; Laboratory of Radiation and Plasmas and Surface Physics (LRPPS); and the Physics Department at the University of Ouargla, Algeria.

Statements & Declarations

All authors declare that this work has been accomplished taking into consideration the ethical and scientific aspect of completing scientific manuscripts, and that all the authors have participated from the scientific side, each according to his field of knowledge, in carrying out this work, and agree for Consent for publication

Funding

The authors declare that no funds, grants, or other support were received during the preparation of this manuscript.

Availability of data and materials

All authors declare that all data and materials are available and declare no Competing interests

Competing Interests

Financial interests: The authors have no relevant financial or non-financial interests to disclose.

Author Contributions

All authors contributed to the study conception and design. Material and simples (rocks) collection and reaparation and the thin films synthesis were done by MEBROUKI Noura. Data collection and analysis were performed by [MEBROKI Noura], [ZENKHRI Louiza] and [BELKHALFA Hakim]. The first draft of the manuscript was written by [MEBROUKI Noura], [ZENKHRI Louiza]. XDR data were interpretated by [MEBROUKI Noura], [ZENKHRI Louiza]. IR spectra and were interpretated by [MEBROUKI Noura], [ZENKHRI Louiza] and [TLILI Salah]. MEB data were interpretated by [MEBROUKI Noura], [ZENKHRI Louiza] and [BOUDJEMA Souhila]. All authors commented on previous versions of the manuscript. All authors read and approved the final manuscript.

References

1. P. S. NAYAK and B. K. SINGH, Instrumental characterization of clay by XRF, XRD and FTIR, Bull. Mater. Sci., 30, 3 (2007).
2. M. M. Sabri, Chemical and structural analysis of rocks using X-ray fluorescence and X-ray diffraction techniques, ARO-Sci. J. K. U., VIII,1, 79 (2020).
3. J. A. Aidekoya, Negative environmental impact of mineral exploitation in Nigeria, Int. J. Phys. Sci., 613 (1995).
4. H. King, Mineral and chemical composition of pure limestone-Missouri Department of Natural Resources., 2005-2015. Geology.com.
5. A. H. Al-Ghamdi, X-ray diffraction and gamma-ray analysis of rock samples from Haradh Region in Saudi Arabia. J. Radia. Res. Appli. Sci., 12, 1 (2019).
6. F. B. Masok, P. L. Masiteng, R. D. Mavunda, P. P. Maleka and H. Winkler, Measurement of radioactivity concentration in soil samples around phosphate rock storage facility in Richards Bay, South Africa. J. Radia. Res. Appli. Sci., 11, 29 (2018).
7. T. Rahman, L. Maxim, Z. Yihuai, B. Ahmed and I. Stefan, Influence of rock microstructure on its electrical properties: an analysis using X-ray microcomputed tomography, 13th International Conference on Greenhouse Gas Control Technologies, 114, 5023 (2017).
8. Z. A. Ahmed, L. Maxim, J. V. Sarah, L. J. Michael, B. Ahmed and I. Stefan, Pore-scale analysis of formation damage in Bentheimer sandstone with in-situ NMR and micro-computed tomography experiments, Journal of Petroleum Science and Engineering, 129, 48 (2015).
9. D. Zandomeneghi, M. Voltolini, L. Mancini, F. Brun, D. Dreossi and M. Polacci, Quantitative analysis of x-ray microtomography images of geomaterials: Application to volcanic rocks, Geosphere, 6 (6), 793 (2010).
10. M. Arif, B. Ahmed, L. Maxim and I. Stefan, Impact of solid surface energy on ettability of CO2/brine/mineral systems as a function of pressure, temperature and salinity, Energy Procedia,114, 4832 (2017).
11. T. Rahman, L. Maxim, B. Ahmed and I. Stefan, Residual trapping of supercritical CO2 in oilwet sandstone, Journal of Colloid and Interface, 469, 63 (2016).

12. I. R. AL-Homadi, I. S. Al-Okli, The Effect of Dolomitization on Mergi Formation Sequences (Cenomanian- Early Turonian) at The Type Section, Northern Iraq. The All-Earth Iraqi National Assembly, Al-Mujjad 18, 1, 149 (2018).
13. T. A. Mirza-Mohammed, Composition and phase mineral variation of Portland cement in Mass Factory Sulaimani – Kurdistan Region NE- Iraq, Int. J. Basic. Appli. Sci. IJBAS-IJENS., 12, (06), 109 (2012).
14. D. A. MCKEOWN and E. P. JEFFREY, Characterization of manganese oxide mineralogy in rock varnish and dendrites using X-ray absorption spectroscopy. *American Mineralogist, 86, 701 (2001).*
15. M. R. Setiawan, M. Iqbal and R. N. Siregar, Mineral analysis in rocks using XRD and Petrography, J. Sci. Applic. Technol., 206 (2018).
16. J.H. Bang, Y.N. Jang, K.S. Song, C.W. Jeon, W. Kim, M.G. Lee and S.J. Park, Effects of sodium laurylsulfate on crystal structure of calcite formed from mixed solutions, J. Coll. Inter. Sci., 356, 1 (2011).
17. W. L. Bragg, F.R.S., Langworthy, Proc. R. Soc. A, 105, 16 (1924).
18. E. N. Caspi, B. Pokroy, P. L. Lee, J. P. Quintana and E. Zolotoyabko, On the structure of aragonite, Acta. Cryst., B61, 129 (2005).
19. E. N. MASLEN, V. A. STRELTSOV and N. R. STRELTSOVA, X-ray Study of the Electron Density in Calcite, CaCO3. Acta Cryst., B49 (132), 636 (1993).
20. [20] S. Miyauchi, H. Imoto and K. Naka, Fabrication of polymer-calcite composite thin films by phase transition of vaterite composite particles with octacarboxy-terminated T8-caged silsesquioxane, Polymer Journal, 48, 1, 1019 (2016).
21. L. B. Gower, Biomimetic model systems for investigating the amorphous precursor pathway and its role in biomineralization. Chem. Rev. 108 (11), 4551(2008).
22. Y. Tanaka, and K. Naka, A carbonate controlled-addition method for size-controlled calcium carbonate spheres by carboxylic acid terminated poly(amidoamine) dendrimers, *Polymer Journal*, 42 (11), 676 (2010).
23. S. M. Antao, H. Ishmael, Temperature dependence of the structural parameters in the transformation of aragonite to calcite, as determined from in situ synchrotron powder X-ray-diffraction data. *The Canadian Mineralogist,* 48 (5), 1225 (*2010).*
24. D. R. Spearing, I. Farnan and J. F. Stebbins, Dynamics of the α-β phase transitions in quartz and cristobalite as observed by in-situ high temperature ^{29}Si and ^{17}O NMR, Phys. Chem. Miner., 19 (86), 307 (1992).
25. B. Mason and L.G. Berry, Elements of mineralogy, A SERIES OF BOOKS IN GEOLOGY, QE363, M37 (1968).
26. H. Okuderaa and A. Hozumi, The formation and growth mechanisms of silica thin film and spherical particles through the Stöber process, Thin Solid Films, 434, 62 (2003).

27. A. C. Genevrier, M. Gich, L. Picas, J. Gazquez, G.L. Drisko, C. Boissiere, D. Grosso, J. R. Carvajal, C. Sanchez, Soft-Chemistry–Based Routes to Epitaxial α-Quartz Thin Films with Tunable Textures, Science 340, 827 (2013).
28. G. L. Drisko, A. C. Genevrier, M. Gich, J. Gàzquez, D. Ferrah, D. Grosso, C. Boissière, J. R. Carvajal and C. Sanchez, Adv. Funct. Mater., 24, 5494 (2014).
29. J. Götze, M. Plötze, T. Graupner, D. K. Hallbauer and C. J. Bray, Trace element incorporation into quartz: a combined study by ICP-MS, electron spin resonance, cathodoluminescence, capillary ion analysis, and gas chromatography, Geo. Cos. Acta., 68 (18), 3741(2004).
30. B. G. Rusk, M. H. Reed, J. H. Dilles and A. J. R. Kent, Intensity of quartz cathodoluminescence and trace-element content in quartz from the porphyry copper deposit at Butte, Montana, Am. Mineral., 91(8-9), 1300 (2006).
31. A. L. Jourdan, T. W. Vennemann, J. Mullis, K. Ramseyer and C. J. Spiers, Evidence of growth and sector zoning in hydrothermal quartz from Alpine veins, Eur. J. Mineral., 21 (1), 219 (2009).
32. K. Lehmann, A. Berger, T. Götte, K. Ramseyer and M. Wiedenbeck, Growth related zonations in authigenic and hydrothermal quartz characterized by SIMS-, EPMA-, SEM-CL- and SEM-CC-imaging, Mineral. Mag., 73 (4), 633 (2009).
33. H. Bambauer, U. Spurenelementgehalte und -Farbzentren in Quarzen aus Zerrklueften der Schweizer Alpen, *Min. Petrogr. Mitt.,* 41, 335 (1961).
34. W. H. Dennen, Trace elements in quartz as indicators of provenance, *Geol. Soc. Am. Bull.,* 78 (1), 125 (1967).
35. Z. Walenczak, Geochemistry of minor elements dispersed in quartz (GE, AL, GA, FE, TI, LI BE), *Arch. Mineral.,* 28 (0002), 190 (1969).
36. V. V. Lyakhovich, Trace Elements in Rock-Forming Minerals of Granitoides (in Russian). Izd. Nedra, Moscow, 200 (1972).
37. H. Fritze, High-temperature piezoelectric crystals and devices, J. Electroceram., 26,122 (2011).
38. G. W. Fox and G. A. FINK, The Piezoelectric Properties of Quartz and Tourmaline, J. Appl. Phys., 5 (10), 302 (1934).
39. M. P. Volarovich and E. I. Parkhomenko, The piezoeffect in rocks, Dokl. AN SSSR., 2, 90 (1954).
40. A. V. Shubnikov, Piezoelectric textures, Moscow-Leningrad : Izd-vo AN USSR, 99 (1946).
41. A. N. NIKITIN and T. I. IVANKINA. On the possible mechanisms of the formation of piezoelectric active rocks with crystallographic textures. Textures and Microstructures., 25, 33 (1995).
42. S. Beddiaf, S. Chihi, Y. Leghrieb, The determination of some crystallographic parameters of quartz, in the sand dunes of Ouargla, Algeria. J Afr Earth Sci., 106, 129 (2015).
43. F. B. Reig, J. V. G. Adelantado, M. C. Moreno, FTIR quantitative analysis of calcium carbonate (calcite) and silica (quartz) mixtures using the constant ratio method. Application to geological samples, Talanta., 58, 811 (2002).

44. JCPDS data Philips X'Pert High Score Package, International Center for Diffraction Data, Newtown Square PA (2011).
45. F. Munawaroh, L. K. Muharrami, T. Kantoro and Z. Arifin. Synthesis and Characterization of Precipitated CaCO3 from Ankerite Prepared by Bubbling Method, ICBSA., 2018, 98 (2019).
46. B. J. Saikia, G. Parthasarathy and N. C. Sarmah, Fourier transforminfrared spectroscopic estimation of crystallinity in SiO2 based rocks, Bull. Mater. Sci., 31(5), 775 (2008).
47. B. F. Pederson, D. Semmingsen, Neutron diffraction refinement of the structure of gypsum, CaSO4 2H2O, Acta. Cryst. Sec., B38, 1074 (1982).
48. *C. YAO, A. XIE, Y. SHEN, J. ZHU and T. LI.* Green Synthesis of Calcium Carbonate with Unusual Morphologies in the Presence of Fruit Extracts, J. Chil. Chem. Soc., 58 (4), 2235 (2013).
49. G. Anbalagan, A. Prabakaran and S. Gunasekaran, Spectroscopic characterization of Indian stander sand, J. Appl. Spect., 77(1), 86 (2010).
50. F. A. Andersen and L. Brecevic, Infrared Spectra of Amorphous and Crystalline Calcium Carbonate, Acta Chem. Scand., 45, 1018 (1991).
51. N. Mahdadi, S. Chihi, H. Bouguettaia, S. Beddiaf and M. L. Mechri, Chromatic classification of Ouargla (Algeria) dunes sand: determination of Main compositions and color causes, by using XRD, FTIR and XRF, Silicon., 9(2), 211 (2017).
52. R. L. Frost, J. T. Kloprogge, Z. Ding, The Garfield and Uley nontronites-an infrared spectroscopic comparison, Spectrochimica. Acta. Part., A58, 1881 (2002).
53. J. Madejova, FTIR techniques in clay mineral studies, Vib. Spectrosc., 31 (1), 1 (2003).
54. B. Hasan, A. Sedat, Ö. E. Serhan, G. Hale and N. C. S. Emine, Quantification of CaCO3–CaSO30.5H2O–CaSO42H2O mixtures by FTIR analysis and its ANN model, Mater. Lett., 58, 723 (2004).
55. Sh. Fu, Q. Lan and J. Yan, Trace element chemistry of hydrothermal quartz and its genetic significance: A case study from the Xikuangshan and Woxi giant Sb deposits in southern China, Ore. Geolo. Rev., 126, 103732 (2020).
56. M. P. Davidson, G. H. Symmes, B. A. Cohen, R. J. Reeder and D. H. Lindsley, Synthesis of the new compound CaFe(CO3)2 and experimental constraints on the (Ca, Fe)CO3 join, Geochimi. Casmochimi. Acta., 57(23-24), 5105 (1993).
57. N. Meftah and M. S. Mahboub, Spectroscopic characterizations of sand dunes minerals of El-Oued (Northeast Algerian Sahara) by FTIR, XRF and XRD analyses, SILICON., 12, 147 (2020).
58. S. Chraibi, H. Moussout, F. Boukhlifi, H. Ahlafi and M. Alami, Utilization of calcined eggshell waste as an adsorbent for the removal of phenol from aqueous solution, J. Encapsulati. Adso. Sci., 6(4), 132 (2016).
59. Y. Liu, H. Xu, and G. Wu, Synthesis of Calcite Superstructures Using Water Reducer as Adjuster, *Chem. Select.*, *5 (31)*, 9709 (2020).

60. F. S. Kodeh, I. M. El-Nahhal, E. A. Elkhair and A. H. Darwish, Synthesis of CaO–Ag-NPs @CaCO3 Nanocomposite via Impregnation of Aqueous Sol Ag-NPs onto Calcined Calcium Oxalate, Chemistry Africa., (2019).
61. J. A. Weil, A review of electron spin spectroscopy and its application to the study of paramagnetic defects in crystalline quartz, Phys. Chem. Miner., 10, 149 (1984).
62. J. A. Weil, A review of the EPR spectroscopy of the point defects in-quartz: The decade 1982–1992, In Physics and Chemistry of SiO2 and the Si-SiO2 Interface., 2, 131 (1993).
63. S. Beddiaf, S. Chihi and Y. Leghrieb, The determination of some crystallographic parameters of quartz, in the sand dunes of Ouargla, Algeria, J. Afr. Earth. Sci., 106, 129 (2015).
64. N. Meftah and M. S. Mahboub, Spectroscopic Characterizations of Sand Dunes Minerals of El-Oued (Northeast Algerian Sahara) by FTIR, XRF and XRD Analyses., Silicon, 2019.
65. P. Scherrer Nachrichten von der Gesellschaft der Wissenschaften zu Göttingen, Mathematisch-Physikalische Klasse., 2, 98 (1918).
66. A. Sdiri, T. Higashi, T. Hatta, F. Jamoussi and N. Tase, Mineralogical and spectroscopic characterization and potential environmental use of limestone from the Abiod formation. Tunisia, Envi. Earth. Sci., 61, 1275 (2010).
67. S. Benchaa, R. Gheriani, A. E. Achouri, H. Bouguettaia and M. L. Mechri, Structural characterizations of dune sand and construction sand of Sidi Slimane and Zaouia El Abidia areas in the Touggourt region in southeast Algeria, Arab. J. Geosci., 14 (2265), 1 (2021).
68. K. Hadjadj, I. Chihi, Rietveld refinement based quantitative phase analysis (QPA) of Ouargla (part of grand erg oriental in Algeria) dunes sand. Silicon., 14, 429 (2020).
69. S. Addala, L. Bouhdjer, A. Chala, A. Bouhdjar, O. Halimi, B. Boudine and M. Sebais, Structural and optical properties of a NaCl single crystal doped with CuO nanocrystals, Chin. Phys., B22 (9), 098103 (2013).

Figures

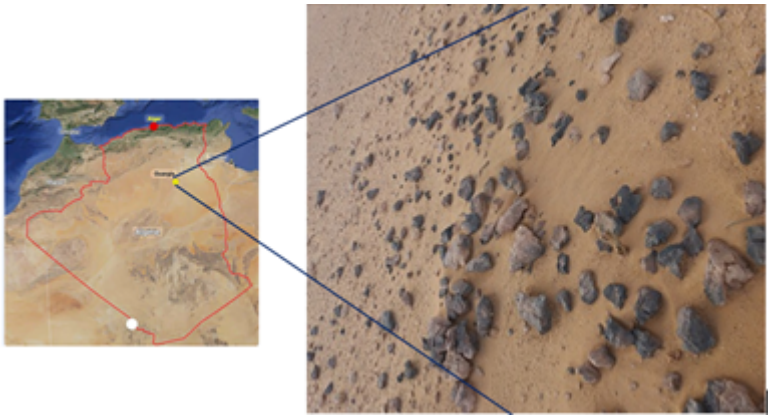

Figure 1

Map of Algeria (http://www.primap.com/wsen/Maps/MapCollection/NationalMaps/Algeria-Satellite-4000x3816.html) showing Ouargla region location and the region from which the analyzed samples are taken.

Figure 2

The samples of studied rocks.

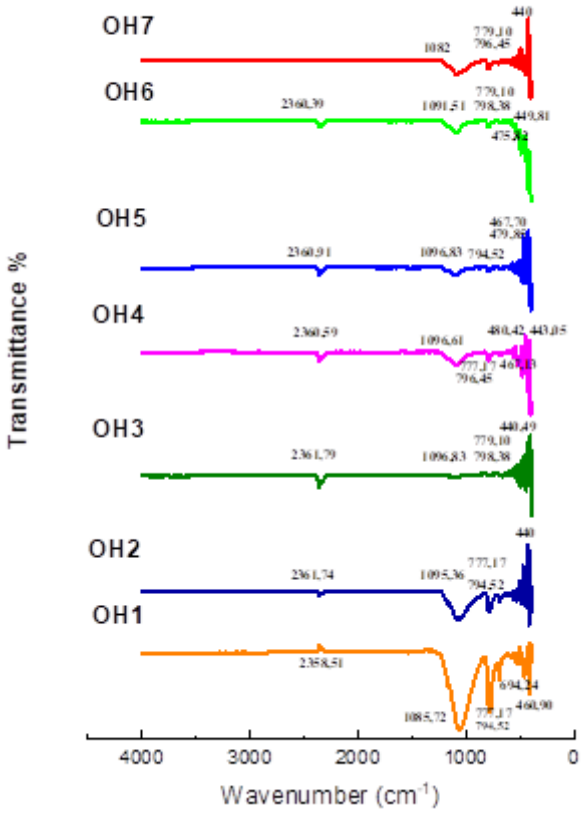

Figure 3

FTIR absorption spectrum of OH sandstones.

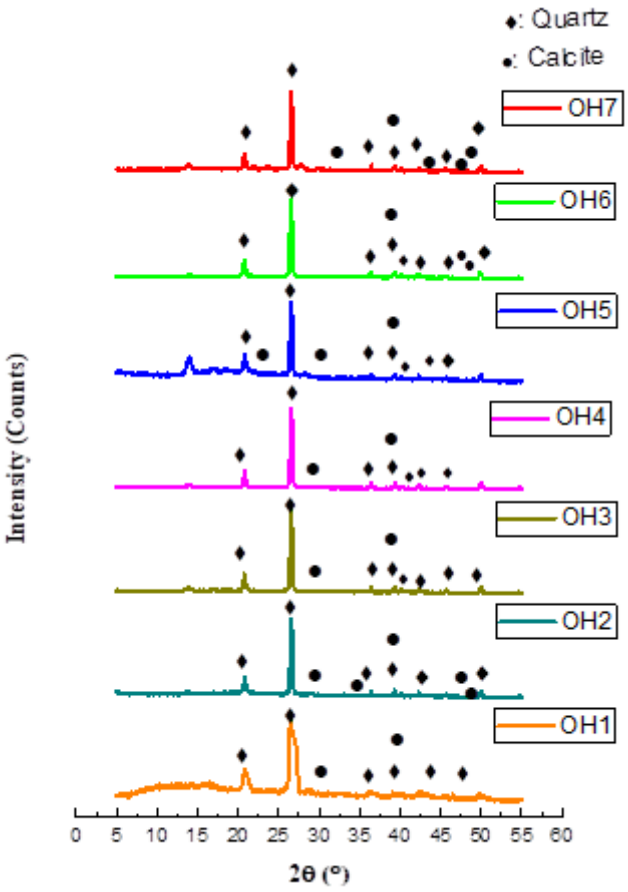

Figure 4

The XRD pattern of OH sandstones.

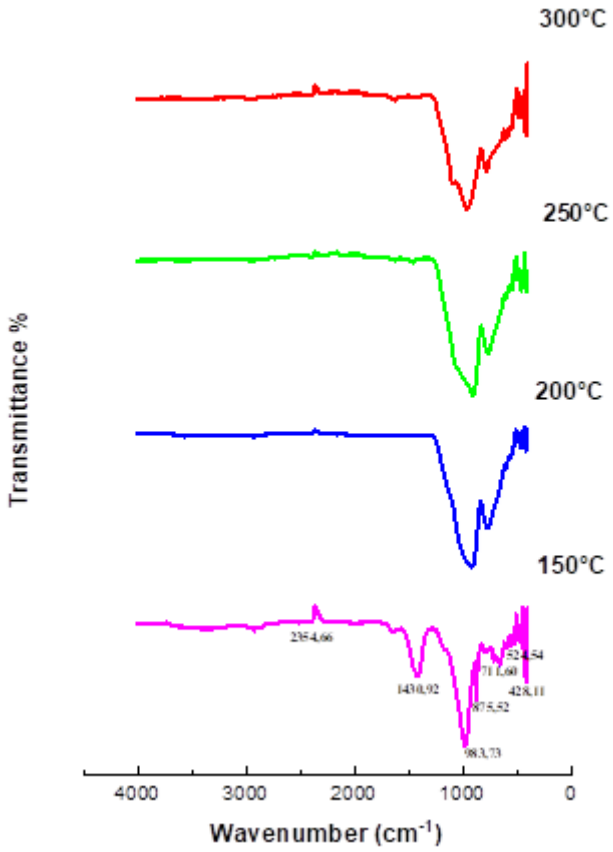

Figure 5

FTIR absorption spectrum of our thin films.

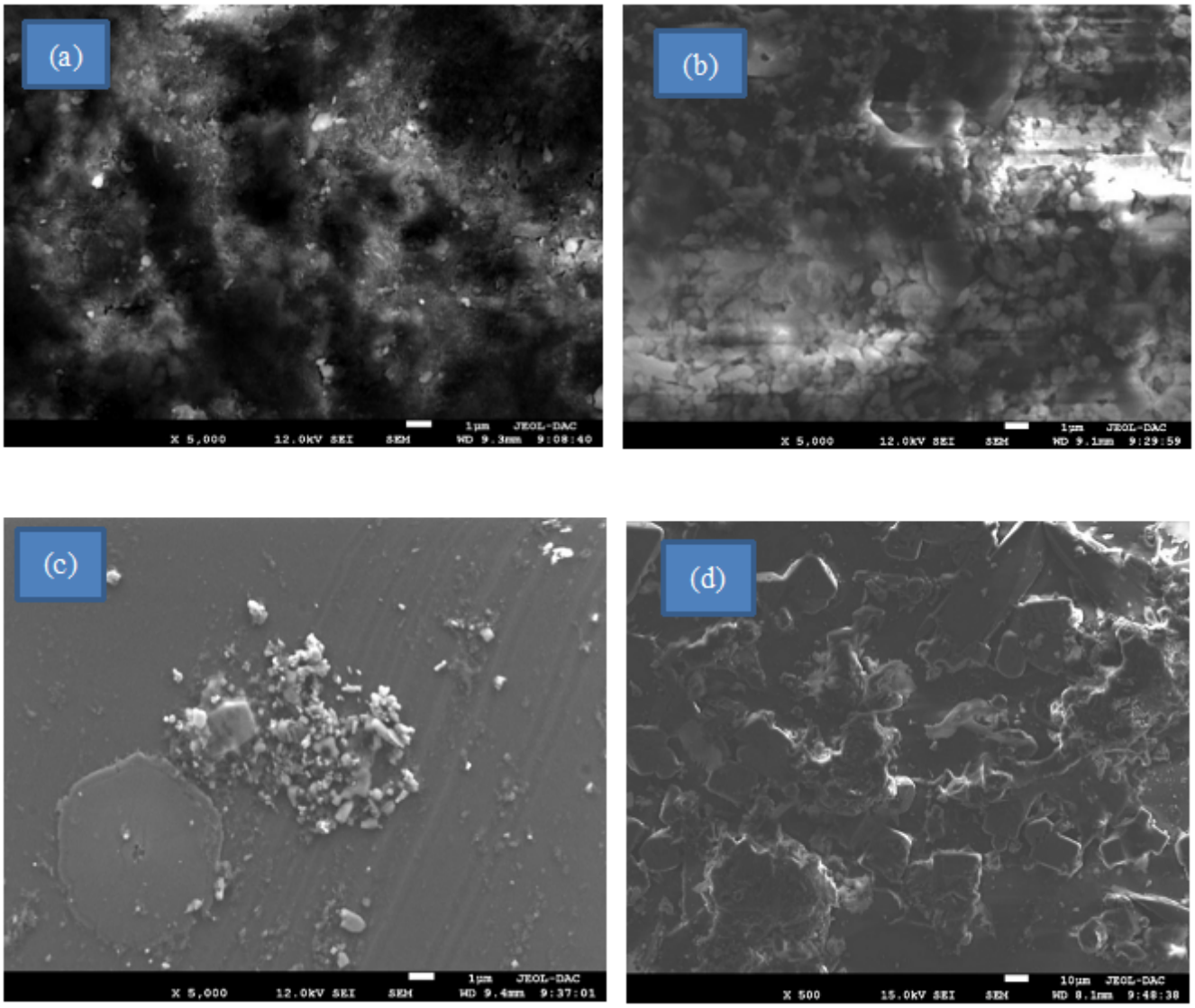

Figure 6

SEM images of thin films at 150 °C (a), 200 °C (b), 250 °C (c) and 300 °C (d).

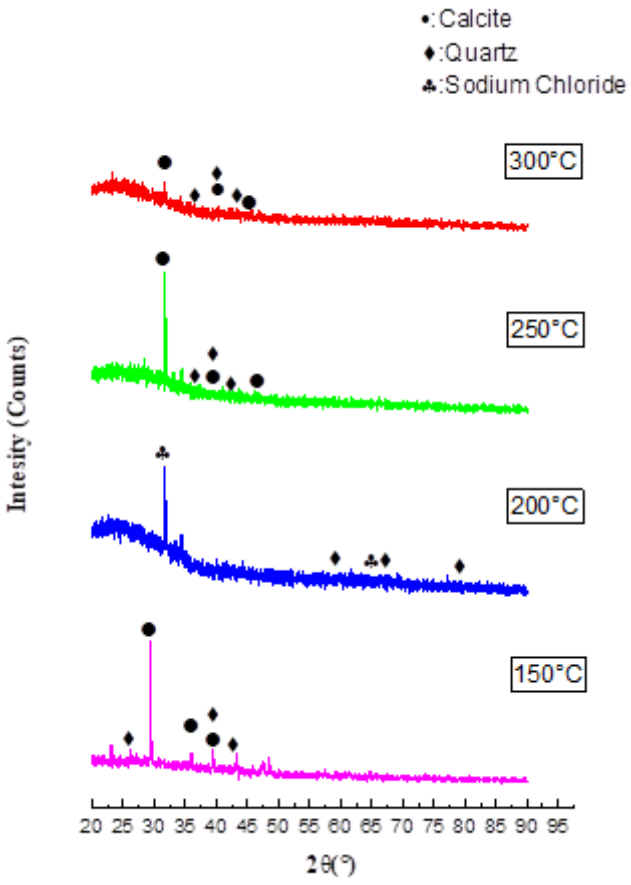

Figure 7

The XRD pattern of our thin films.